IL NUOVO CIMENTO Vol. 34 C, N. 6 Novembre-Dicembre 2011
DOI 10.1393/ncc/i2011-11088-3

Colloquia: IFAE 2011

Searches for rare B decays with missing energy at SuperB

E. Manoni(*)

INFN, Sezione di Perugia - Perugia, Italy

(ricevuto il 29 Luglio 2011; pubblicato online il 21 Dicembre 2011)

Summary. — We present the current experimental status and the perspectives at SuperB on the searches for rare B decays with missing energy in the final state. Experimental improvements due to the detector design will be illustrated. The expected constraints on parameters entering New Physics models will also be discussed.

PACS 13.20.He – Decays of bottom mesons.
PACS 13.25.Hw – Decays of bottom mesons.

1. – Thoretical motivations

Rare B decay measurements may be used as probe for indirect searches for physics beyond the Standard Model (SM) and represent a complementary approach to direct New Physics (NP) searches performed at LHC. Of particular interest are B decays with undetectable neutrinos in the final states, for whose search e^+e^- colliders, as SuperB will be, are the optimal environment.

1˙1. $B \to K^{(*)}\nu\overline{\nu}$. – Processes mediated by flavor changing neutral currents, as $B \to K^{(*)}\nu\overline{\nu}$, are forbidden at tree level in the SM. They happen through W-box or Z-penguin diagrams as shown in fig. 1 (left and central plots). As discussed in ref. [1], in the operator product expansion framework, the effective Hamiltonian governing the quark-level $b \to s\nu\overline{\nu}$ transition is: $\mathcal{H} = \frac{4G_F}{\sqrt{2}} V_{tb}V_{ts}^*(\mathcal{C}_L^\nu \mathcal{O}_L^\nu + \mathcal{C}_R^\nu \mathcal{O}_R^\nu)$, G_F being the Fermi constant, V_{ij} the CKM matrix elements, and $\mathcal{C}_{L(R)}^\nu$ the Wilson coefficients associated to the left (right)-handed operators $\mathcal{O}_{L(R)}^\nu$. Experimental quantities, such as inclusive and exclusive $b \to s\nu\overline{\nu}$ branching fractions and the fraction of longitudinally polarized K^* in the

(*) Work supported by Fondazione Cassa di Risparmio di Perugia, Progetti Ricerca di Base "La fisica del sapore nell'era di LHC", Codice Progetto:2009.010.0438.

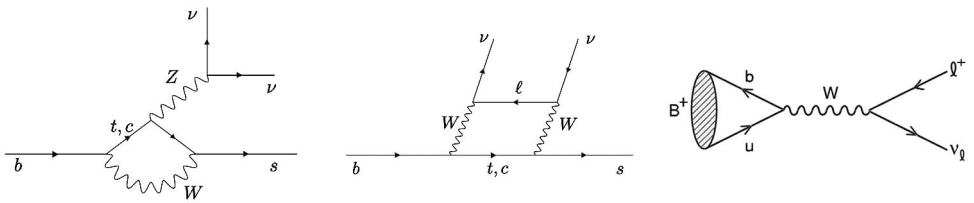

Fig. 1. – (Colour on-line) Leading-order SM diagrams for $b \to s\nu\overline{\nu}$ (left and center) and $B \to \ell\nu_\ell$ (right).

$B \to K^*\nu\overline{\nu}$ decay, may be expressed as a function of the Wilson coefficients:

$$\mathcal{B}(B \to X_s\nu\overline{\nu}) = 2.7 \times 10^{-5} \times (1 + 0.09\eta)\epsilon^2, \tag{1a}$$

$$\mathcal{B}(B \to K\nu\overline{\nu}) = (4.5 \pm 0.7) \times 10^{-6} \times (1 - 2\eta)\epsilon^2, \tag{1b}$$

$$\mathcal{B}(B \to K^*\nu\overline{\nu}) = (6.8 \pm 1.1) \times 10^{-6} \times (1 + 1.31\eta)\epsilon^2, \tag{1c}$$

$$F_L(B \to K^*\nu\overline{\nu}) = (0.54 \pm 0.01) \times (1 + 2\eta)/(1 + 1.31\eta) \tag{1d}$$

having defined $\epsilon = \sqrt{|C_L^\nu| + |C_R^\nu|}/|(C_L^\nu)^{SM}|$ and $\eta = -Re(C_L^\nu C_R^{\nu *})/(|C_L^\nu|^2 + |C_R^\nu|)$. Figure 2 (left plot) shows the hypothetical constraints on the (ϵ, η)-plane assuming infinite experimental precision and assuming the SM predictions for the central values ($C_R^{\nu SM} \simeq 0$, $C_L^{\nu SM} = -6.38 \pm 0.06$). NP models predict the presence of non-standard particles in the Z-loop or new sources of missing energy which can modify the Wilson coefficients and, as a consequence, the experimental observable.

1˙2. $B \to \tau\nu$. – As shown in fig. 1 (right plot), in the SM the $B \to \tau\nu$ transition happens through a W-mediated annihilation diagram and the branching fraction is given by

$$\mathcal{B}(B \to \tau\nu) = \frac{G_F^2 m_B m_\ell^2}{8\pi}\left(1 - \frac{m_\ell^2}{m_B^2}\right)^2 f_B^2 \left|V_{ub}\right|^2 \tau_b = (1.20 \pm 0.20) \times 10^{-4}, \tag{2}$$

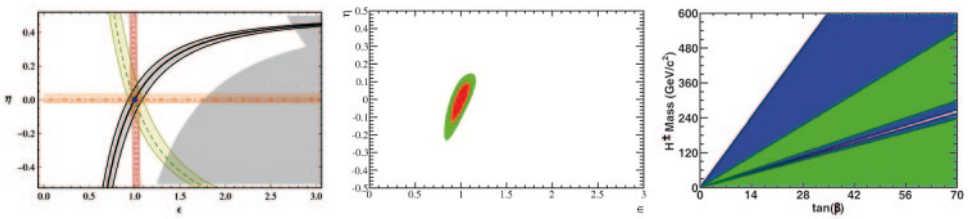

Fig. 2. – (Colour on-line) Left: hypothetical constraints on the (ϵ, η)-plane, considering theory uncertainties only. The green band (dashed line) represents $\mathcal{B}(B \to K^*\nu\overline{\nu})$, the black band (solid line) $\mathcal{B}(B \to K\nu\overline{\nu})$, the red band (dotted line) $\mathcal{B}(B \to X_s\nu\overline{\nu})$ and the orange band (dot-dashed line) $\langle F_L \rangle$. The shaded area is ruled out experimentally at the 90% confidence level. Center: expected constraint on the (ϵ, η)-plane, from the SuperB measurement of $\mathcal{B}(B \to K^{(*)}\nu\overline{\nu})$ and the angular analysis of $B^0 \to K^{*0}\nu\overline{\nu}$ at $75\,\mathrm{ab}^{-1}$. Right: excluded region at 95% confidence level in m_{H^+} *vs.* $\tan\beta$ plane from the HFAG world average for $\mathcal{B}(B \to \tau\nu)$ (green, small bands) and from the $75\,\mathrm{ab}^{-1}$ SuperB measurement (blue, large bands).

where the numerical value is obtained using V_{ub}, the decay constant f_B, and the B lifetime τ_B as in refs. [2, 3], and [4], respectively. In models which predict the existence of a charged Higgs, *i.e.* 2-Higgs Doublet Model (2HDM) [5], the W may be replaced by a H^+ and, depending on the value of $\tan\beta$, the interference between the two diagrams may be constructive or destructive. The ratio between the 2HDM and the SM prediction for the branching fraction is $(1 - \tan^2\beta m_B^2/m_H^2)^2$. Comparing the SM expectation with the experimental results, regions on the $(m_H, \tan\beta)$-plane can be excluded.

2. – Analysis technique and current experimental status

From the experimental point of view, searches for rare B decays can be performed at the flavour factories by exploiting the so-called "recoil method". At the center-of-mass energy corresponding to the $\Upsilon(4S)$ mass, $B\overline{B}$ pairs may be produced. One of the two B's ($B_{\rm reco}$) is reconstructed in hadronic or semileptonic final states. The aim is to collect as many as possible B candidates to study the recoil properties. The algorithm starts from a $D^{(*)}$ meson to whom a high-momentum light lepton or a hadronic system consisting of up to 6 kaons and/or pions both charged and neutrals is added. The semileptonic (SL) $B_{\rm reco}$ reconstruction comprises 18 reconstructed modes, while the hadronic (HAD) algorithm collects more than 1000 final states. The first has a higher reconstruction efficiency, given the higher final state branching fraction, while the HAD method benefits from a lower contamination from mis-reconstructed candidates due to the completely closed kinematics. Once the $B_{\rm reco}$ has been identified, the remaining tracks and neutrals are used to search for the signal signature ($B_{\rm sig}$), *i.e.* a kaon (or a kaon plus a pion for the K^* mode) or a τ lepton accompanied by missing energy associated to the undetectable neutrino(s). Kinematic and event shape variables are exploited at selection stage. A veto on additional charged tracks is imposed, while the sum of the neutral energy not used in the $B_{\rm reco}$ nor in the $B_{\rm sig}$ reconstruction ($E_{\rm extra}$) is one of the most powerful variables. In fact the $E_{\rm extra}$ distribution is expected to peak at zero for correctly reconstructed events, while it should assume higher values for combinatoric $B_{\rm reco} - B_{\rm sig}$ pairs. This is used in the final steps of the analysis to extract the signal yield, by fitting the $E_{\rm extra}$ distribution or defining a tight signal window once all the other selection criteria have been applied. Given the fact that, apart from the undetected neutrinos, all the other final products in the event are reconstructed and the state produced by the e^+e^- collision is well know, a powerful kinematic constraint can be imposed to compute both the missing energy and $E_{\rm extra}$. This makes the recoil method the most powerful strategy to search for $B \to K^{(*)}\nu\overline{\nu}$ and $B \to \tau\nu$ and is not feasible at hadronic machines. Table I reports the current experimental knowledge for the quantities under investigation and the results used to compute the expected sensitivity at SuperB. The uncertainty in the measurements is dominated by the statistical error, the systematic part is mainly due to the limited statistics of the simulation sample used to estimate the signal efficiency and to model the distribution of the variables used in the event yield estimation. For $\mathcal{B}(B \to \tau\nu)$ non–statistical-in-origin systematics are present and will be important at the SuperB high luminosity.

3. – Expected sensitivity at SuperB and phenomenological constraints

To estimate the expected sensitivity after 5 years of SuperB data taking, corresponding to $75\,{\rm ab}^{-1}$, we started from the BaBar analysis, given the similarity between the BaBar and SuperB detectors. In fact, the baseline design for the latter, is inspired to the

TABLE I. – *Current experimental knowledge for $\mathcal{B}(B \to K^{(*)}\nu\overline{\nu})$ and $\mathcal{B}(B \to \tau\nu)$ and analysis used to compute the expected sensitivity at SuperB.*

Channel	Statistics (fb^{-1})	Measurement
$B^+ \to K^+\nu\overline{\nu}$	492	$\mathcal{B} < 1.4 \times 10^{-5}$ [6](*)
$B^+ \to K^+\nu\overline{\nu}$	418	$\mathcal{B} < 5.6 \times 10^{-5}$ [7](°)
$B^+ \to K^{*+}\nu\overline{\nu}$	413	$\mathcal{B} < 8.0 \times 10^{-5}$ [8](*)(°)
$B^0 \to K^{*0}\nu\overline{\nu}$	413	$\mathcal{B} < 12.0 \times 10^{-5}$ [8](*)(°)
$B^+ \to \tau^+\nu$	1,023	$\mathcal{B} = (1.64 \pm 0.34) \times 10^{-4}$ [2](*)
$B^+ \to \tau^+\nu$	426	$\mathcal{B} = (1.80^{+0.57}_{-054}(\text{stat}) \pm 0.26(\text{syst})) \times 10^{-4}$ [9](°)

(*) Most precise measurement.
(°) Used for SuperB extrapolation.

BaBar detector and will partially reuse some of its pieces. The addition of two optional subdetectors, namely a particle identification device in the forward region (FWD PID) and a calorimeter in the backward region (BWD EMC), are under study [10]. We applied a cut-and-count analysis *à la* BaBar and we used the SuperB simulation tools to evaluate the change in signal efficiency and background rejection. Taking the BaBar results for event yield, normalization and signal efficiency, rescaling for the luminosity and accounting for the changes in efficiencies, we estimated the SuperB sensitivities. The responsibles for the improvement in signal selection and background rejection are:

– lower beam boost with respect to BaBar [11]: +20% reconstruction efficiency for both correctely and wrongly reconstructed event, −10% background efficiency when applying the extra tracks veto due to higher detector hermeticity;

– FWD PID: +2.5–5% gain in signal efficiency and unchanged background efficiency due to improved kaon identification;

– BWD EMC: −2%(−15%) selection efficiency for signal (background) due to the use of the calorimeter as a veto device.

Simulated experiments have been performed to evaluate the sensitivity at different luminosities. The study has been performed considering three different configurations: BaBar boost and detector layout ("BaBar" configuration), SuperB boost and baseline SuperB detector ("SuperB" configuration), SuperB boost and SuperB detector with FWD PID and BWD EMC ("SuperB + options" configuration).

In table II the statistics needed to have a 3σ evidence for the $B \to K^{(*)}\nu\overline{\nu}$ channels are reported. It can be noticed that the biggest improvement is due to the reduced boost which traslates in a higher detector hermeticity and reconstruction efficiency. The effect of having the two optional SuperB detectors is also non-negligible. Simulated experiments have also been performed to evaluate the sensitivity of an angular analysis for the $B \to K^*\nu\overline{\nu}$ channel [12]. The expected sensitivity on the observable F_L at $75\,\text{ab}^{-1}$ is expected to be around 50%. The F_L, $\mathcal{B}(B^+ \to K^+\nu\overline{\nu})$ and $\mathcal{B}(B \to K^*\nu\overline{\nu})$ results may be combined to determine preferred regions in the (η, ϵ)-plane. Figure 1 (central plot)

TABLE II. – *Needed statistics for the 3σ evidence for $B \to K^{(*)}\nu\overline{\nu}$ in three different configurations, described in the text. The last column lists the expected sensitivity at $75\,\mathrm{ab}^{-1}$ considering the SuperB + options configuration.*

Channel	BaBar	SuperB	Superb + options	$75\,\mathrm{ab}^{-1}$ sensitivity
$B^+ \to K^+\nu\overline{\nu}$	$8\,\mathrm{ab}^{-1}$	$5\,\mathrm{ab}^{-1}$	$4\,\mathrm{ab}^{-1}$	10%
$B \to K^*\nu\overline{\nu}$	$75\,\mathrm{ab}^{-1}$	$50\,\mathrm{ab}^{-1}$	$42\,\mathrm{ab}^{-1}$	25%

shows the results of the phenomenological analysis done by considering the $75\,\mathrm{ab}^{-1}$ error on the three experimental quantities listed above and the SM expectation as central value. As discussed in ref. [1], a model with a potential non-vanishing C_R^ν term would lead to a non-crossing of the experimental bands in the (η, ϵ)-plane and a band for F_L far from zero. Given the SuperB sensitivity at $75\,\mathrm{ab}^{-1}$, this model may be discarded or well distinguished from the SM, depending on the measured central values.

For the $B \to \tau\nu$ search, considering the latest BaBar measurement [9], the branching fraction is known with a precision of 35%, of which 32% due to statistical error and 15% to systematic effects. Part of the systematics (12.1%) is statistical in origin, the remaining portion (7.4%) will not scale with luminosity and has been conservatively treated as an irreducible source of uncertainty. With this recipe, the $75\,\mathrm{ab}^{-1}$ expected sensitivity on $\mathcal{B}(B \to \tau\nu)$ has been computed to be 7% considering the HAD recoil only and 5% adding also the SL analysis. At very high luminosity (some tens of ab^{-1}), the systematic contribution to the error dominates and analysis improvements will be required to further reduce the experimental uncertainty. Assuming the SM predicted central value for the branching fraction and the SuperB sensitivity at $75\,\mathrm{ab}^{-1}$ considering both SL and HAD analysis, constraints on the Higgs mass-$\tan\beta$ plane have been set, as shown in fig. 1 (right plot): the blue (small) bands correspond to the most stringent branching fraction measurement from HFAG with an associated uncertainties of 20%, the green (large) bands have been set by considering the 5% accuracy at SuperB. The constraint coming from the SuperB result on $\mathcal{B}(B \to \tau\nu)$ is competitive with the ones from other measurements in the flavour sector [13] and will be complementary to the charged Higgs searches at LHC.

4. – Conclusions

It has been discussed as rare B decays with undetectable particles in the final state represent a probe for indirect NP searches. SuperB represents an optimal ground where to search for them. Preliminary results on the SuperB sensitivity have been shown. The $75\,\mathrm{ab}^{-1}$ collectable after 5 years of data taking will allow to determine $\mathcal{B}(B \to \tau\nu)$ and $\mathcal{B}(B \to K^{(*)}\nu\overline{\nu})$ with 7% and 30% precision, respectively. This will provide stringent constraints on parameters entering different NP models that will be discarded or confirmed, considering also the interplay with other measurements in the flavour sector and with direct searches from LHC.

REFERENCES

[1] Altmannshofer W., Buras A. J., Straub D. M. and Wick M., *JHEP*, **0904** (2009) 022.
[2] Heavy Flavor Averaging Group, `http://www.slac.stanford.edu/xorg/hfag/index.html`.
[3] Gamiz E. *et al.* (HPQCD Collaboration), *Phys. Rev. D*, **80** (2009) 014503.
[4] Nakamura K. *et al.* (Particle Data Group), *J. Phys. G*, **37** (2010) 075021.
[5] Hou W.-S., *Phys. Rev. D*, **48** (1993) 2342.
[6] Chen K.-F. *et al.* (BELLE Collaboration), *Phys. Rev. Lett.*, **99** (2007) 221802.
[7] del Amo Sanchez P. *et al.* (BABAR Collaboration), *Phys. Rev. D*, **82** (2010) 112002.
[8] Aubert B. *et al.* (BABAR Collaboration), *Phys. Rev. D*, **78** (2008) 072007.
[9] del Amo Sanchez P. *et al.* (BABAR Collaboration), [arXiv:1008.0104 [hep-ex]].
[10] Grauges E. *et al.* (SuperB Collaboration), [arXiv:1007.4241 [physics.ins-det]].
[11] Biagini M. E. *et al.* (SuperB Collaboration), [arXiv:1009.6178 [physics.acc-ph]].
[12] O'Leary B. and (SuperB Collaboration), [arXiv:1008.1541 [hep-ex]].
[13] Haisch U., [arXiv:0805.2141 [hep-ph]].